

# Self-Sustained Collective Oscillation Generated in an Array of Non-Oscillatory Cells

Yue Ma\* and Kenichi Yoshikawa†

*Spatio-Temporal Order Project, ICORP, Japan Science and Technology Agency (JST)*

*Department of Physics, Graduate School of Science, Kyoto University, Japan*

(Dated: June 21, 2024)

Oscillations represent a ubiquitous phenomenon in biological systems. The conventional models of biological periodic oscillations are usually proposed as interconnecting transcriptional feedback loops. Some specific proteins function as transcription factors, which in turn negatively regulate the expression of the genes that encode those “clock protein”. These loops may lead to rhythmic changes in gene expression of a cell. In the case of multi-cellular tissue, the collective oscillation is often obtained from synchronization of these cells, which manifest themselves as autonomous oscillators. In contrast, here, we propose a different scenario for the occurrence of collective oscillation in a multi-cellular system independent of oscillation, neither intrinsically oscillatory cells nor periodic external stimulation. It is a coupling induced oscillation, with the consideration of wave propagation due to the intracellular communication.

PACS numbers: A PACS will be appear here

## I. INTRODUCTION

Oscillation is ubiquitous in nature, not only in physics and chemistry but also biology. Biological oscillations can be observed in a wide range of time and population scales, from circadian rhythm about 24 hours [1] to segmentation clock less than 2 hours [2], from whole body oscillatory fevers [3] to periodic protein production in a single cell [4]. Correspondingly, there are a great number of theoretical models. Despite of the diversity of biological insights, there are common points regarding the models.

Proteins are produced from the transcription and translation process of the specific sequence fraction of DNA. On the other hand, proteins can bind to a transcription promotor on DNA and hence repress or enhance its expression. The transcriptional negative feedback loop [5, 6] and the delay [7, 8] in the inner cellular gene-protein network are considered as crucial roles contributing to oscillatory expression of DNA and protein production. From the view point of dynamical systems, such oscillations are limit cycles generated from Hopf bifurcation by choosing appropriate parameter set. Consequently, in the case of cell group or multi-cellular organism with oscillatory character, such as cardiac tissue and segmentation clock in tail of PSM (Presomitic Mesoderm), synchronization of coupled oscillators is often used to explain the observed collective oscillation [9, 10, 11].

However periodic oscillation is only a small part of dynamical behavior for a cell. Oscillation may cease if condition is changed. And in fact, most cells tend to settle down to a seeming stable state. Most recent studies suggest that negative transcriptional feedback is neither

sufficient nor even necessary in some cases, for circadian oscillation, which is the most well studied biological oscillation model. Instead, the intracellular signaling, such as  $\text{Ca}^{2+}$  and cAMP, integrating with transcriptional feedback plays a key role in the long-term circadian pace-making [12]. So, we doubt about the indispensability of intrinsic oscillatory cells in an oscillatory organism. In this paper, we propose a novel mechanism for oscillation to take place in a group of cell. Different from conventional mechanism of synchronized oscillators, none of individual cells in our model is intrinsic oscillatory. The collective oscillation is generated from the intracellular coupling and wave propagation.

We consider the cells are excitable and described by FitzHugh-Nagumo (FHN) equations. The coupled FHN model is a well studied paradigm for excitable medium, in the context of chemical oscillator, computational neuroscience and so on. Oscillating pattern can be usually obtained by setting parameters beyond a Hopf bifurcation. In this paper, however, we focus our attention on another possible scenario, i.e., occurrence of oscillation from non-oscillatory, bistable system. To induce oscillation in a bistable system oscillate, people usually give a periodic stimulate [13] or couple with a oscillatory boundary [14]. But for systems completely independent of oscillating elements, little attention has been paid to their emergence of oscillation.

A few studies in the context of mathematics and physics have revealed the possibility of collective oscillating pattern. The first example was proposed by Smale [15], who found two “dead” cells become “alive” via diffusively coupling. Long after that, more literatures [16, 17] studied detail conditions on this behavior. In-phase and anti-phase self-sustained oscillation on excitable membrane via bulk coupling are observed in [18]. The models under consideration are mostly coupled identical excitable cells with mono-stability. On the other hand, in a bistable system, a stationary front can bifurcate to a pair of fronts propagating in opposite directions.

\*Electronic address: dr.mayue@gmail.com; Corresponding author

†Electronic address: yoshikaw@scphys.kyoto-u.ac.jp

It is known as nonequilibrium Ising-Bloch (NIB) bifurcation [19, 20]. Perturbation for happening NIB bifurcation can be induced by local spatial inhomogeneity [21]. More global analysis showed that NIB point is only part of the story, and conclude that unstable wave front is intrinsic to media that are spatially inhomogeneous [22, 23]. An unstable wave front may manifest itself as reflected front, tango wave [24], pacemaker [25] and so on. In this paper, we will discover new ways of thinking about them beyond mathematics and physics, and extend the its application to biological oscillator.

Moreover, although most studies have been performed on a spatial continuum described by partial differential equations (PDE), continuum models neglect the effects of cellular discreteness [26]. Actually, from the viewpoint of biology, the size of cells can not decrease infinitely. This intrinsic property is difficult to be ignored specially in the stage of initial development in an organism, when cell size is comparable with tissue's. Moreover, there are mathematical reasons to explore the system dynamics with spatial discretization. PDE and ODE (ordinary differential equations) are of different theoretical framework, and produce different results. Several significant features of discreteness, such as wave propagation failure [27], can not happen in a continuum model. Therefore, in this paper, we will use the spatially discrete cell array as the subject, and discuss the impact of discreteness.

## II. DESCRIPTION OF THE MODEL

### A. One dimensional cellular array

In this paper, we consider the cells in one-dimensional space. Cells are coupled by intracellular signaling molecules, which flow trough channels of membrane via concentration difference or depolarization-mediated flux. Intracellular small-molecule signal then integrates with transcriptional feedback loops of adjacent cells. We assume that coupling signal is regulated by the expression of activator  $u$  and interacts neighborhoods in a diffusion-like manner. Including an inhibitor, a one-dimensional array of  $N$  cells can be described as

$$\dot{u}_i = f(u_i, v_i, \Gamma_i) + \tilde{D}(u_{i-1} + u_{i+1} - 2u_i) \quad (1)$$

$$\dot{v}_i = g(u_i, v_i) \quad (2)$$

where  $i \in \{1 \dots N\}$  the index of the cell in the chain,  $\tilde{D}$  the coupling strength of  $u$ .  $f$  and  $g$  are reaction functions of activator and inhibitor, respectively. The boundary condition is zero flux, i.e.,  $u_0 = u_1$  and  $u_N = u_{N+1}$ .  $\Gamma_i$  is an environmental parameter, which discussed in detail later.

Note that only coupling of activator is involved in this study. For most of models studying pattern formation, diffusion is assumed to be occurred for every elements. Specially, a much larger diffusion of inhibitor is necessary for inducing Turing instability [28]. Cells membrane, however, is very selective on passing substance.

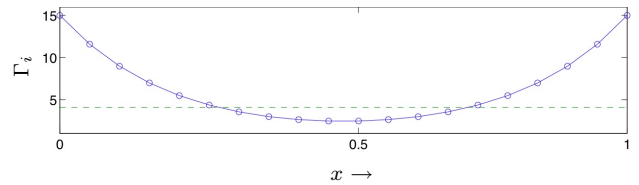


FIG. 1: Profile of  $\Gamma_i$ , when  $\Gamma_0 = 15, \xi = 5$ .

Usually, complicate intracellular reactions take place locally, but triggered by only one or a small number of specific signaling molecules. For example, the segmentation clock involves cyclic expression of many gene, but the crucial pathway for coupling is only via the transmembrane receptor Notch1 [29]. Thus, in the context of biology, we only consider the coupling between activator, and inhibitor in our model is no more than a local state variable.

### B. Active factor

The development of a multicellular organism begins with a single cell, which divides and give rise to different typologies of cell. Different cells are organized according to certain secreted chemicals, called morphogens. Despite improvement of the experimental and theoretical approach, the mechanisms of the morphogenesis have remained unclear. Usually, morphogens are considered to be produced in specific sites and diffuse over the organism [30]. Quite recently, evidence of “shuttling-based” mechanism has been presented [31]. The key of the models are going to define a robust and scaling profile, usually a concentration gradients, of morphogens. Thinking broader, we can suppose there are some environmental parameters behave as the morphogens. Environment, in which organism arise, supply nutrition for growth, in such a way that directly contact border get more and far inside cells get less.

In this paper, we pay no attention to any specific chemical substance, just suppose that there is a certain factor, which we refer to active factor, to provide the information between position and cell dynamics.

Without losing generality, we assume that the active factor  $\Gamma$  is constant at boundaries of organism. It diffuses into the organism field at the diffusion constant  $D_a$ , and is degraded at rate  $\alpha$ . Thus we have

$$\frac{\partial \Gamma}{\partial t} = D_a \frac{\partial^2 \Gamma}{\partial x^2} - \alpha \Gamma. \quad (3)$$

Because our model is based on coupled ODEs independent from spatial variation, the profile of active factor satisfies scaling property. Normalizing the field size to 1, we can get a steady profile ( $\partial \Gamma / \partial t = 0$ ) of  $\Gamma$  as

$$\Gamma(x) = \frac{\Gamma_0}{e^{-\xi} - e^{\xi}} ((e^{-\xi} - 1)e^{\xi x} - (e^{\xi} - 1)e^{-\xi x}), \quad (4)$$

where  $\Gamma_0 = \Gamma(0) = \Gamma(1)$  is the value at two boundaries, and  $\xi = 1/\lambda = \sqrt{\alpha/D_a}$  is inverse of the decay length. A typical profile of  $\Gamma(x)$  is shown as Fig. 1. Blue circles indicate the value of  $\Gamma$  of discrete cells ( $N = 20$  in the figure) laid uniformly in the scaling field.

### C. Bistability

Above mentioned active factors can affect the fate of cells in a concentration dependent manner [32]. We assume that cells tend to live in a stable state normally, and high concentration of active factor can excite the cell to another stable state. This kind of bistability is very important and has been observed in various biological systems, such as cell signaling and neural process [33, 34, 35]. Moreover, it was recently suggested that stochastic fluctuation plays an important role on the manner of transition between bistable states [36].

Usually, the bistability takes place from positive genetic regulation loops [34, 37, 38]. Conventional biochemical theory clarified a key-lock relationship between transcription factor and promoter. In this paper, however, we shed light on a physical regulation of protein production, which has been ignored improperly by biochemists, and consider the bistability in a broader way. A DNA molecule that is longer than several micrometers (over 100 000 base pairs) shows the characteristics of a semi-flexible polymer, which exhibits a discrete transition between coiled and compact states; i.e., a first-order phase transition for a single giant DNA molecule. The discrete transaction leads to the ON/OFF switching of DNA transcription, and hence the production specific protein [39]. In this transition process, the specific key-lock interaction helps little, and instead the transition is induced by “nonspecific” interaction between a DNA molecule and environmental factors within the cell, such as the concentration of polyamine, mRNA, ATP, and so forth [39, 40, 41]. Moreover, RNA [42], protein [43] and other molecules [44] are also found discrete switch between folding and unfolding or between active and inactive state. Although the details of the mechanism has yet to be clarified, it is believed to play an important role in self-regulation of gene expression in living cells, and might be a more universal law of morphogenesis pattern than other biochemical reactions.

The ON/OFF switching character of DNA molecular suggests that its free energy  $F$ , which is a measure of higher order structure, is a double minimum kinetic. Without losing generality, we assume the kinetic is of quartic, as shown in Fig. 2(a), with respect to specific field parameters  $\eta$ , such as density. Usually, it stays in either OFF or ON corresponding to the intracellular concentration of nonspecific abundant chemical species, such as ATP, polyamines, small ions, etc. Consequently, the state of DNA's higher order structure, either coiled or compact, then effects the processes of transcription. In the scale of molecular, since the ef-

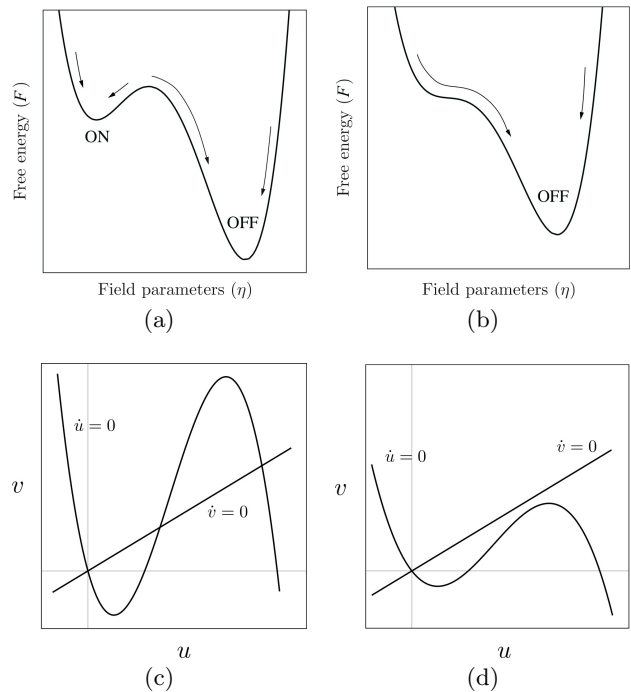


FIG. 2: Free energy (a & b) and nullcline diagrams (c & d) in the situation of bistability (a & c) and mono-stability (b & d), respectively.

fect of inertia can be ignored comparing with viscosity, the change of density is in a ratio of generalized force, so we have  $\partial\eta/\partial t \sim -\partial F/\partial\eta$ . Clearly, due to the assumption of quartic kinetic of  $F$ ,  $-\partial F/\partial\eta$  turns to be a cubic function. With above considerations, we choose the reaction function of every single cell as the form of FitzHugh-Nagumo (FHN) equations. Moreover, we can determine an active factor as a certain signaling protein, such as ComK in soil bacterium to develop “competence” event [36], or chemicals in intracellular environment, such as mRNA, ATP, etc. [39, 40, 41]. We suppose that cells with high concentration of active factor are capable of bistability switching between OFF and ON, as shown in Fig. 2(a), while cells with low concentration of it can only behave OFF state, as shown in Fig. 2(b).

Including an inhibitor, the dynamical reaction function of every single cell can be described as

$$\dot{u} = f(u, v, \Gamma) = \Gamma u(u - \alpha)(1 - u) - v \quad (5)$$

$$\dot{v} = g(u, v) = \epsilon(\beta u - v) \quad (6)$$

where  $u$  a variable relating to the activity of DNA,  $v$  the inhibitor changing slowly compare to  $u$  in the case of  $\epsilon \ll 1$ . Throughout this paper, following parameters are fixed as

$$\alpha = 0.3, \beta = 0.5, \epsilon = 0.02. \quad (7)$$

Fig. 2(c)&(d) show the nullclines with bistability and mono-stability on the condition that  $\Gamma$  is large and small, respectively. Specifically, with above parameters, the

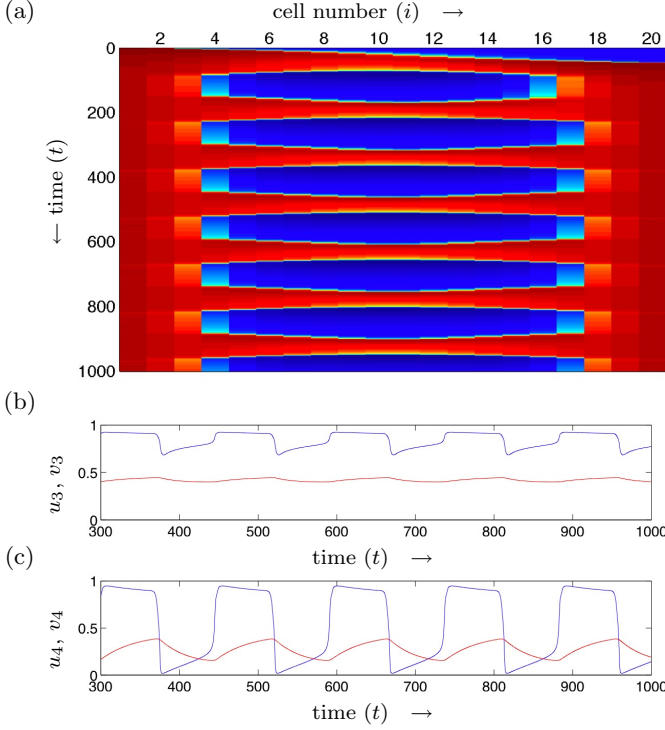


FIG. 3: Collective oscillation observed in a chain of cell when  $\tilde{D} = 0.7$ . (a) Spatio-temporal plot of the collective oscillation of  $u_i$ . Color red and blue indicate  $u_i = 1$  and  $u_i = 0$ , respectively. (b, c) Waveform of  $u$  (blue) and  $v$  (red) in 3rd and 4th cell.

critical value of  $\Gamma$ , which separate two kinds of stability, is 4.08. Thus, in case of the spatial profile of  $\Gamma_i$  as shown in Fig. 1, only central 8 cells ( $7^{th}$  -  $14^{th}$ ) are mono-stable, while others are bistable. Again, there is no oscillatory cell with the absence of coupling.

Substituting Eq. 5&6 into Eq. 1&2, we get the system equations used in this paper.

$$\dot{u}_i = \Gamma_i u_i (u_i - \alpha)(1 - u_i) - v_i \quad (8)$$

$$+ \tilde{D}(u_{i-1} + u_{i+1} - 2u_i) \quad (9)$$

$$\dot{v}_i = \epsilon(\beta u_i - v_i)$$

We change the coupling strength  $\tilde{D}$  and observe the occurrence, variation and disappearance of self-sustained collective oscillation in the cell array.

### III. SELF-SUSTAINED COLLECTIVE OSCILLATION

#### A. Normal collective oscillation

Fig. 3(a) shows a typical oscillation when coupling strength  $\tilde{D} = 0.7$ . An enlarged view of one period of oscillation is shown in Fig. 4(a). As the initial condition, we set the 1st cell excited, because of the general trend

that a stimulate usually inputs from the border. At the beginning ( $0 < t \lesssim 80$ ), a traveling wave appears due to the excitation on the border. Then the traveling front sweeps over the cell array and make all the cells excited (see Fig. 4(b)). Although central cells are also turned on due to the influence of interaction, they can not stay at the excitable state for a long time. Instead, they tend to return to their stable equilibrium soon (see Fig. 4(c)), and hence generate two counterpropagating wave backs, as shown in Fig. 4(d). These two wave backs propagate outward until the  $3^{rd}$  and  $18^{th}$  cell and stop suddenly due to the spatially discreteness (see Fig. 4(e)). The “wall” cells do not jump from ON state to OFF state and remain a small amplitude oscillation. As an example, the difference between  $3^{rd}$  and  $4^{th}$  cell is shown in Fig. 3(b, c). At this critical interface, the inhibitor  $v$  slowly decreases so that the  $4^{th}$  and  $17^{th}$  cells restore excitability after a while. Then central cells can be inspired again by the pair of reflecting wave front, as shown in Fig. 4(f). Pushed by the wave, central cells will be excited again. This process repeats and causes the collective oscillation inside the multi-cell tissue without oscillatory cells.

#### B. Stationary state before birth of oscillation

Above collective oscillation can be observed when coupling strength is larger than a threshold, below which the *wave backs* (see Fig. 4(d)) fail to reflect, and remain the state as Fig. 4(e). A spatio-temporal diagram is shown in Fig. 5, in which the central cells stay silent while excited bands appear close two borders.

Note that it is impossible that this phenomena take place in a continuum counterpart. The existence of coupling strength threshold under which wave propagation failure happens is special for spatial discrete system. Actually, there is another threshold, which is even smaller, for *wave front* to stop propagating. In that case, the excited signal at border fail to propagate forward, but we do not discuss it in this paper.

#### C. In-phase and anti-phase period doubling oscillation closed to boundary

By increasing the coupling strength  $\tilde{D}$ , property of the oscillation can be changed. In Fig. 6, we show that the position of oscillation shift periodically. The  $3^{rd}$  and  $18^{th}$  cells oscillate with a doubled period, in anti-phase (Fig. 6(b,c)). Globally, tissue oscillates in two groups with the same cell population but different position: No. 3-No. 17 (15 cells) and No. 4-No. 18 (15 cells), respectively.

Interestingly, increasing the coupling strength  $\tilde{D}$  a little more, say  $\tilde{D} = 0.9$ , we found a different type of period-doubling, as shown in Fig. 7. To compare with the case of  $\tilde{D} = 0.8$ , although the critical interface between ON and OFF shifts periodically like Fig. 6, there is no phase

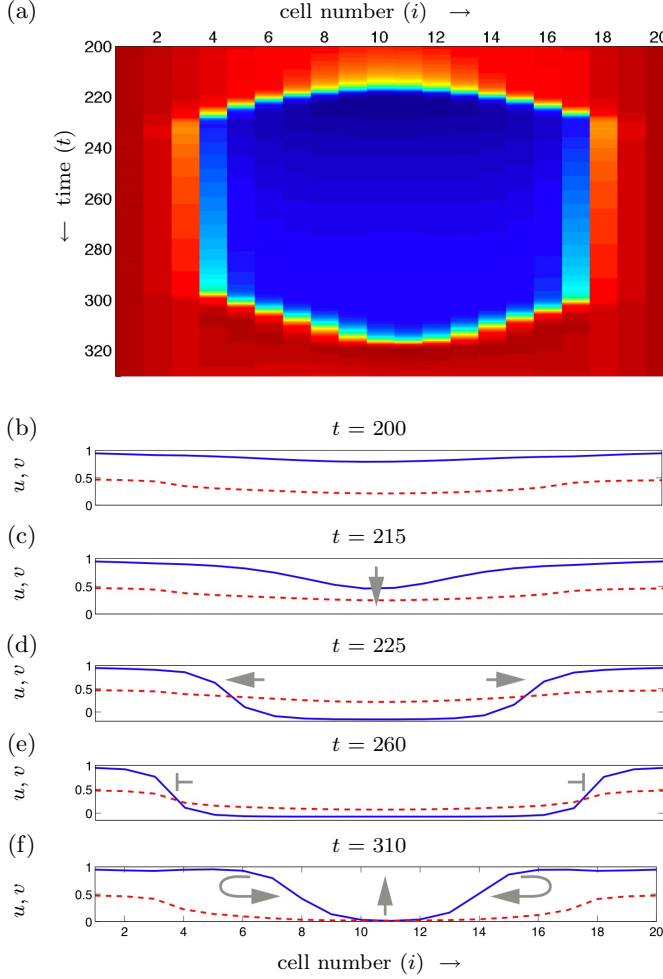


FIG. 4: (a) A spatio-temporal diagram of  $u_i$  in one period, (b)-(f) Snapshots of  $u$  and  $v$  at several time point in one period. It illustrates the change of wave propagation in different stages. Blue solid curves and red dashed curves indicate  $u$  and  $v$ , respectively.

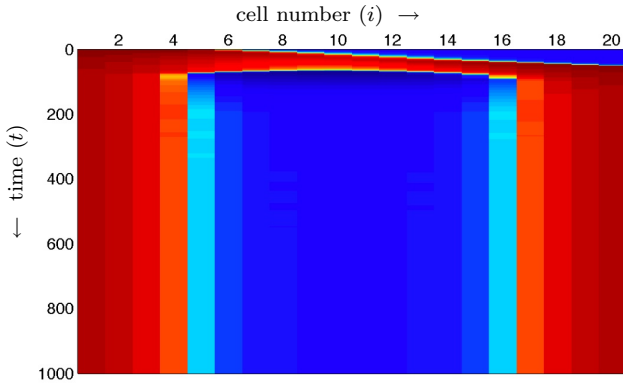


FIG. 5: Spatio-temporal diagram of  $u_i$  on stationary state. The wave propagation stops and no oscillation occurs in the weak coupling case  $\tilde{D} = 0.47$ .

difference between 3<sup>rd</sup> and 18<sup>th</sup> cell. As shown clearly in

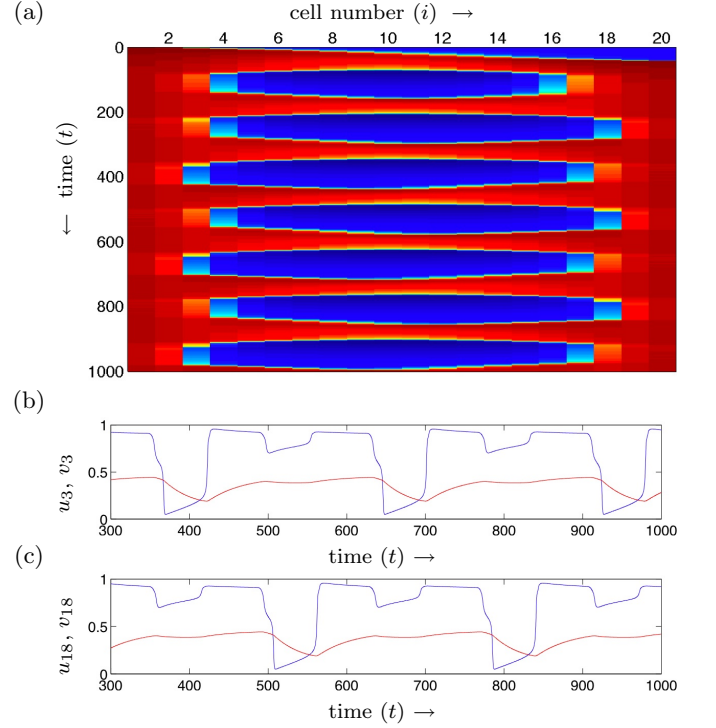


FIG. 6: Anti-phase mode in the period doubling produces collective oscillation with periodic position shift when  $\tilde{D} = 0.8$ . (a) Spatio-temporal diagram of  $u_i$ . Color red and blue indicate  $u_i = 1$  and  $u_i = 0$ , respectively. (b) and (c) are waveform diagrams of 3rd and 18th cell. Activator  $u$  and inhibitor  $v$  are colored in blue and red, respectively.

their waveform (Fig. 7(b,c)), these two boundary cells oscillate in-phase, instead of anti-phase (Fig. 6(b,c)). Therefore in present condition, the periodic change does not take place on the oscillating position, what changed is the population of oscillating cells instead. Precisely speaking, tissue oscillate in two groups: No. 3-No. 18 (16 cells) and No. 4-No. 17 (14 cells), respectively.

Moreover, setting the initial condition of single cells identically, i.e., all in ON state at  $t = 0$ , we have checked that same symmetric collective oscillation can also occur in the case of  $\tilde{D} = 0.8$ . So we conclude that these two types of oscillation are caused by same Hopf bifurcation. Because the larger  $\tilde{D}$  is, the faster wavefront propagates, a larger coupling strength can reduce the time lag between two boundary cells being inspired. If the time lag is smaller, two boundary converge to an in-phase oscillation. On the other hand, if it is big, they will behave as anti-phase oscillation.

#### D. Oscillation death

Increasing coupling strength  $\tilde{D}$ , we observed that the periodic position or population change stop, and the normal oscillation returns. But comparing to the case of

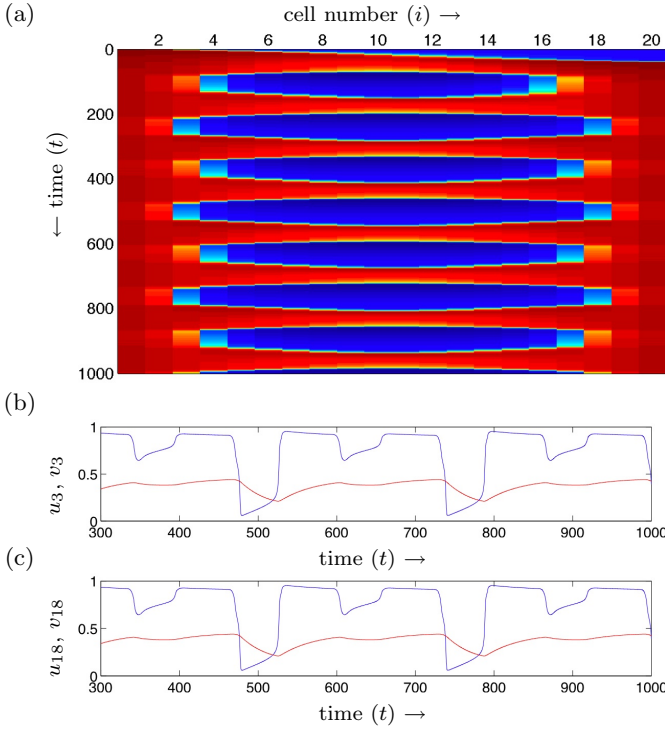


FIG. 7: In-phase mode in the period doubling produce collective oscillation with periodic population change when  $\tilde{D} = 0.9$ . (a) Spatio-temporal diagram of  $u_i$ . Color red and blue indicate  $u_i = 1$  and  $u_i = 0$ , respectively. (b) and (c) are wave-form diagrams of 3<sup>rd</sup> and 18<sup>th</sup> cell. Activator  $u$  and inhibitor  $v$  are colored in blue and red, respectively.

$\tilde{D} = 0.7$ , the total population of oscillating cells increase to 16 (No. 3 to No. 18) from 14 (No. 4 to No. 17).

A sudden death of the oscillation occurs when  $\tilde{D}$  is as large as 2.6. From Fig. 8(b), one can tell clearly that central cells start to oscillate after all cells are excited, but this oscillation is unsustainable. In this strong coupling condition, the boundary cells can not recover their excitability so that the propagating wave front from center is unable to stop and reflect to generate successive oscillation.

Before the oscillation death happens, there is a narrow parameter region  $2.53 \leq \tilde{D} \leq 2.56$ , where only one side of the “wall” alternatively collapses, and a complicated period-4 collective oscillation is observed (Fig. 8(a)).

### E. An overall look

Here, we sweep the coupling strength  $\tilde{D}$  from 0.45 to 2.7, and summarize the variation of oscillation period and the (left) border position of oscillation region. Fig. 9(a) shows the diagram of the cell number of the left boundary of collective oscillation. If coupling strength is smaller than 0.48, there is no oscillation, and 4 cells from tissue border are excited while cells 5–16 are silent. Oscillation

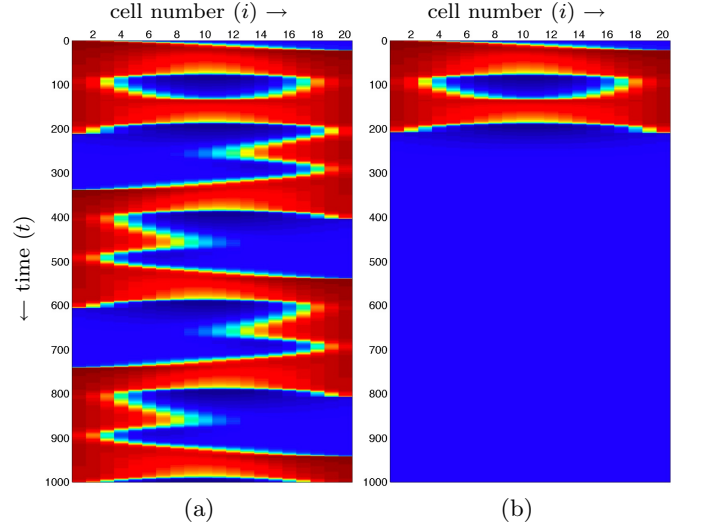


FIG. 8: Spatio-temporal diagram of  $u_i$ . Color red and blue indicate  $u_i = 1$  and  $u_i = 0$ , respectively. (a)  $\tilde{D} = 2.53$ , oscillation starts to collapse; (b)  $\tilde{D} = 2.6$ , oscillation ceases after one cycle.

takes place when wave back passes 4<sup>th</sup> cell at  $\tilde{D} = 0.48$ . Then the border shifts between 3 and 4, while in-phase and anti-phase period doubled oscillation occur, between  $0.78 < \tilde{D} < 0.97$ . Finally, the oscillation gets its maximum region: cells from 3 to 18, until  $\tilde{D}$  is too large to occur oscillation.

Variations of oscillation period are shown in Fig. 9(b). Once the central cells start to collectively oscillate, its period decrease rapidly when coupling strength increases. The rate of period decrease slows down gradually. The period changes little in the region where  $\tilde{D}$  is large. This phenomena happens because the stationary interval (Fig. 4(e)) contributes greatly to the period of oscillation. The shrink of stationary interval shorten the oscillation period significantly when  $\tilde{D}$  is small. When  $\tilde{D}$  is large enough, however, the wave backs reflect immediately without stop, and the period turns to be determined mainly by propagating velocity.

There is a parameter region (light gray) in which system manifests itself as period two oscillation with in-phase or anti-phase character (initial condition dependent). Although we denote the critical parameter value as PD, it is not a Period-Doubling bifurcation in traditional sense, which generate a pattern of alternatively shorter and longer periodic. We will do more detailed investigation on this kind of spatio-temporal bifurcation phenomena in our future work.

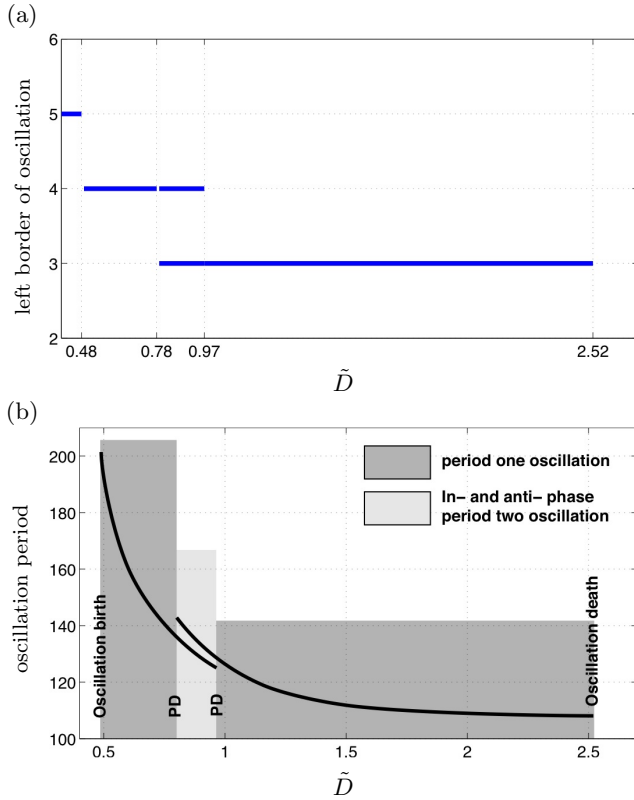


FIG. 9: Phase diagram describing (a) position (the index of cell) of left border of oscillation and (b) the oscillation period, with the change of coupling strength.

## IV. DISCUSSION

### A. Discreteness v.s. continuum

Above phenomena are observed in a spatially discrete system. As briefly introduced in Sec I, the discreteness is important in both mathematical and biological sense. We are going to discuss this significance in more detail.

The diffusion term  $D(\partial^2 u / \partial x^2)$  in a one dimensional spatial continuous reaction-diffusion model can be formulated as  $D(u_{i-1} + u_{i+1} - 2u_i) / \Delta x^2$  in its difference version. This type of conversion is a common approach to solve PDE numerically. The diffusive rate  $D$  usually do not change much for a specific substance in a constant condition. But the coupling strength  $\tilde{D}$  we used in previous sections tends to be changed by various molecular biological factors. We assume, however, the coupling is mainly due to the diffusion like effects of substances,  $\tilde{D}$  is approximate to  $D / \Delta x^2$ . Since the profile of active factor has the scaling property, it is reasonable to suppose the gradient works for any size of field. Then we study how the change of field effects global dynamics.

During the initial period of development, cells have enough space to increase its population. Thus the distance between cells  $\Delta x$  is so loose that  $\tilde{D}$  is possible a relative small value. Therefore, at the beginning, the cell

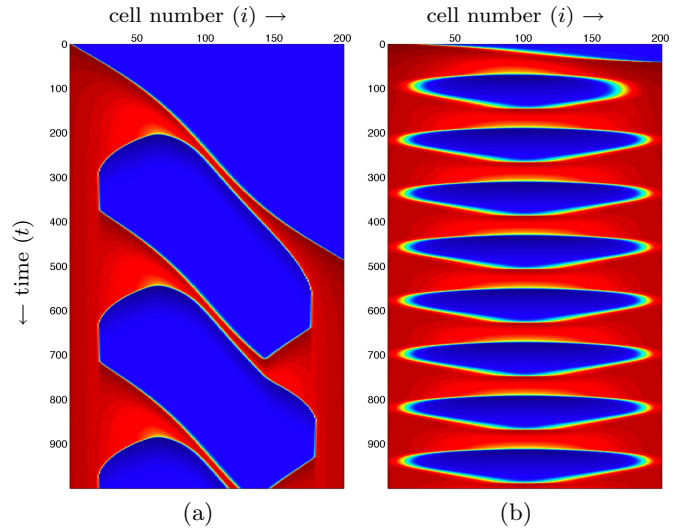


FIG. 10: Spatio-temporal diagram of  $u_i$ . Color red and blue indicate  $u_i = 1$  and  $u_i = 0$ , respectively.  $N = 200$ . (a) The case that cells grow in an open field,  $\tilde{D} = D / \Delta x^2 = 0.7$ . (b) The case that cells grow in a limited field,  $\tilde{D} = D / \Delta x^2 = 70$ .

group may not be observed oscillation, but only divided into several functional “layers”, just as shown in Fig. 5. As cell division goes on and population grows, cells may get compacted. Decrease of  $\Delta x$  results larger coupling strength  $\tilde{D}$ , and collective oscillation may start to take place.

If the field in which cells continue to grow is open or large enough,  $\Delta x$  and  $\tilde{D}$  will not significantly change. We draw the spatio-temporal diagrams with number of cells becoming 10 times more,  $N = 200$ , in Fig. 10(a). Other parameters are same with those in Fig. 3. Obviously, it takes longer time for wave sweep over the organism. Period of the oscillation and phase difference between two sides increases greatly.

On the other hand, if the cell population increases in a limited space, the distance  $\Delta x$  between cells become smaller and smaller, and the system manifests itself more like a continuum rather than a discrete system. In this case, coupling strength will increase dramatically in the square order with respect to the decrease of  $\Delta x$ . Suppose that the field has been just filled up when  $N = 20$ , then 10 times of  $N$  will result 100 times of  $\tilde{D}$ . That means  $\tilde{D}$  is as large as 70, if  $N = 200$ . Under this condition, we have the spatio-temporal diagram given in Fig. 10(b). Comparing with Fig. 3, the period of the collective oscillation changes little. It suggests that the clock runs punctually, in case that the size of organism does not grow,

In the mathematical sense, when population of cells is big enough in a fixed field, the behavior of organism will follow the solution of a specific partial differential equation, which is independent of the number of cells.

Moreover, during one period of Fig. 10(b), there is no such sudden stop of wave front and stationary interval as Fig. 4(a). Thus, the period of oscillation will be eval-

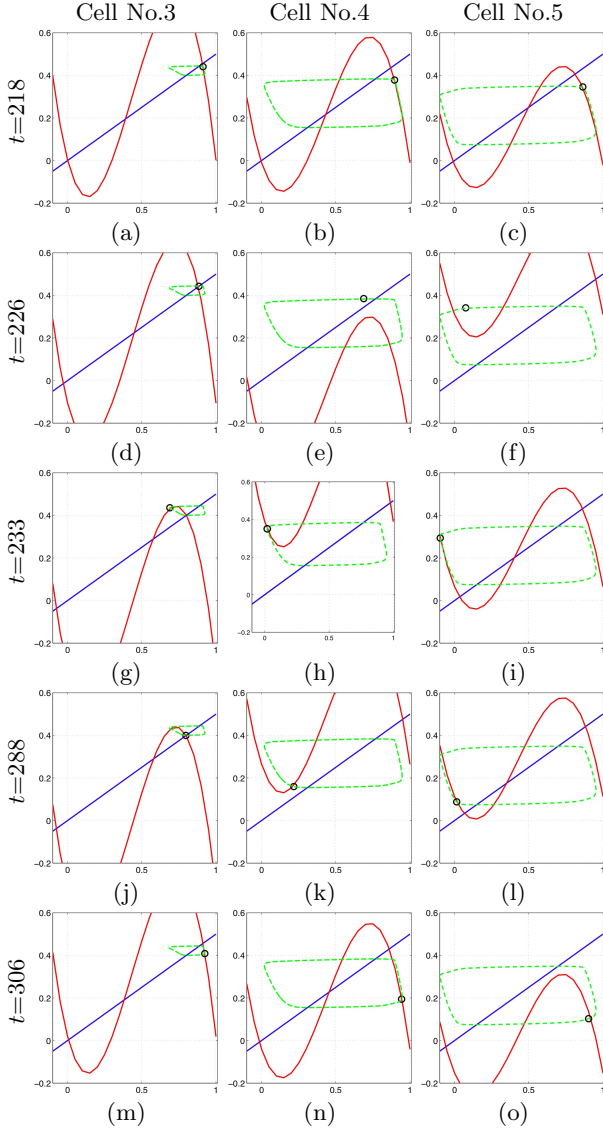


FIG. 11: Phase portrait diagrams with the snapshots of dynamical nullcline. Rows indicate the time evolution from top down, and columns indicate the number of cells (3 at left, 4 at middle and 5 at right). Green dashed curves are limit cycle solution. Red cubic function curves are the nullcline of  $\dot{u}_i = 0$ . Blue straight lines are nullcline of  $\dot{v}_i = 0$ . Blue circles are position of  $(u_i, v_i)$  at specific time.

uated mainly by wave propagation speed in the limited field case and stationary duration in the open field case, respectively.

### B. Understanding the mechanism

The occurrence of the self-sustained collective oscillation is caused by the excitability of cells and the mutual interaction. Complicated bifurcation are involved in the system. We are going to give some qualitative ideas on how the oscillation takes place.

From dynamical equations (5,6) and their nullcline illustrated in Fig. 2(c,d), we know that single cell may manifest itself as bistability or mono-stability. By inducing the effect of coupling, however, the nullcline of one cell will dynamically change according to states of its neighbors and itself. Because we assume that the communication between cells is only mediated via the activator  $u$ , the strict nullcline  $\dot{v}_i = 0$  is independent from coupling.

$$v_i = G(u_i) = \beta u_i. \quad (10)$$

From Eq.(1)&(5), we get the function of nullcline  $\dot{u}_i = 0$  as

$$v_i = F(u_i, \Gamma_i) = \Gamma_i u_i (u_i - \alpha)(1 - u_i) + \Delta U_i, \quad (11)$$

where  $\Delta U_i = \tilde{D}(u_{i+1} + u_{i-1} - 2u_i)$  the offset of cubic function due to the coupling. Thus, nullcline  $v = F(\cdot)$  is dynamically moved up and down in phase plane, corresponding to the state of  $u_{i-1}, u_i, u_{i+1}$ .

In Fig. 11, we show the phase portrait of cells around the oscillating border (cells No.3-5), as well as their dynamical nullcline at some turning points. Snapshots are taken under the same conditions of normal oscillation as shown in Fig. 3.

The first row of Fig. 11 are state of all excited, i.e.,  $u_i$  of all three cells are close to 1. So, under this condition, the vertical offset  $\Delta U$  of nullcline is nearly zero, and all of three cells are of bistability. Then the second row is taken at  $t = 226$ , when the wave back comes (see Fig. 4(d)), and the 3<sup>rd</sup> cell moves towards its lower equilibrium (Fig. 11(f)). Because  $\Delta U_4 = \tilde{D}(u_3 + u_5 - 2u_4)$ , a sudden drop of  $u_5$  leads to a quick sink of cubic nullcline. Shown in Fig. 11(e), the red cubic nullcline moves down so that the higher equilibrium disappears. In a word, the 4<sup>th</sup> cell turns to be mono-stable and state converge quickly to the left branch of cubic nullcline. As time goes on, the drop of  $u_4$  makes nullcline of the 3<sup>rd</sup> cell moves down. But because the 3<sup>rd</sup> cell has a larger  $\Gamma$ , which controls the amplitude of cubic nullcline, even if  $u_4$  decrease to its lowest value (Fig. 11(h)), i.e.,  $\Delta U_3$  reduces to its minimum, the cross points between cubic and straight nullcline still remain. It is just the reason why the wave back can pass the 4<sup>th</sup> cell, but stops at the 3<sup>rd</sup> cell (Fig. 4(a)). After the stop of propagation, there is a relatively long stationary period from time 230 to 300. In this interval, the inhibitor  $v_4$  reduces slowly. Because  $u_3 \approx 1$  and  $u_5 \approx 0$ ,  $\Delta U_4$  is so big that the cubic nullcline is above the straight one (Fig. 11(k)). Under this condition, the cell is a mono-stable with the equilibrium at the right branch of cubic function. Thus, after a while, the state of  $u$  will switch to the higher value (Fig. 11(n)), and inspires a reflecting wave (Fig. 4(f)). Note that a smaller coupling strength  $\tilde{D}$  leads to a smaller offset  $\Delta U$ . If we move down the cubic nullcline a little bit to cross the straight nullcline in Fig. 11(k), the 4<sup>th</sup> cell turns to be bistable. That will disable the switch from left to right, and stop the oscillation (Fig. 5).

From above description and Fig. 11, we conclude that the boundary cell, which is bistable without coupling, turns to switching between two types of mono-stable dynamics. This switching becomes the power of self-sustained oscillation observed in present model. The variation of offset of dynamical nullcline of the boundary cell gives rise to rich oscillation phenomena.

### C. Conditions for occurring oscillation

Here, we are going to explore the condition of oscillation in an approximate manner by studying the dynamics on the border, where the wave backs (WB) stop, and wave fronts (WF) generate. Investigating the dynamical nullcline and state variable, we concluded that a wave back will not pass a critical cell  $c$ , if there still exist cross points between nullclines when cell  $c+1$  has dropped to its lower equilibrium (Fig. 11(g,h)). On the contrast, if the cross points disappear, state of  $u_c$  will switch to lower equilibrium and cell  $c$  is possible to oscillate (Fig. 11(e,f)). Similarly, to fire a wave front, two nullclines of an edge cell can not cross when the state of inhibitor recovery to its lower limit.

Thus, we can roughly solve the condition by finding two possible tangency points of two nullclines Eq. (10) and Eq. (11). It can be obtained from following equations:

$$\frac{dF(u, \Gamma)}{du} = \frac{dG(u)}{du}, \quad (12)$$

Eq. 12 is the condition for two nullclines having the same slope. Substituting  $F$  and  $G$  into Eq. 12, we have

$$\Gamma(-3u^2 + 2(1 + \alpha)u - \alpha) = \beta, \quad (13)$$

from which we get two solutions

$$u_{T1,2} = \frac{13 \pm \sqrt{79 - 150/\Gamma}}{30}. \quad (14)$$

For cell  $c$  propagating the wave back, there should have only lower equilibrium when  $u_c$  close to the higher tangency point. The corresponding condition is  $F(u_{T1}, \Gamma_c) < G(u_{T1})$ , Substitution leads to

$$\Gamma_c u_{T1} (u_{T1} - \alpha)(1 - u_{T1}) + \tilde{D}(u_{c-1} + u_{c+1} - 2u_{T1}) < \beta u_{T1}. \quad (15)$$

On the other hand, for cell  $c$  to generate wave front, there should have no lower equilibrium when  $u_c$  close to the lower tangency point. It simply means  $F(u_{T2}, \Gamma_c) > G(u_{T2})$ , which can be rewritten as

$$\Gamma_c u_{T2} (u_{T2} - \alpha)(1 - u_{T2}) + \tilde{D}(u_{c-1} + u_{c+1} - 2u_{T2}) > \beta u_{T2}. \quad (16)$$

Two critical conditions are illustrated in Fig. 12.

*Approximation*

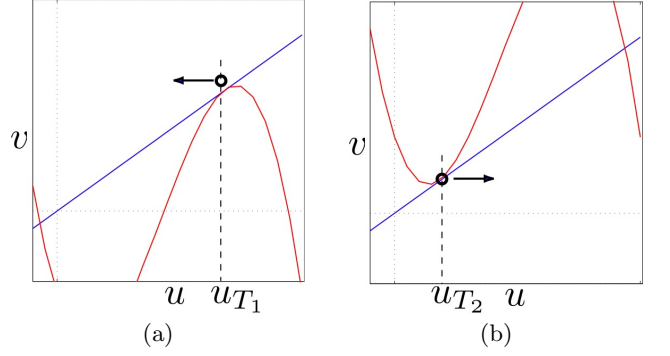


FIG. 12: Schematic diagram for illustrating two critical tangency situations, corresponding to the conditions on which (a) wave back passes and (b) wave front is generated.

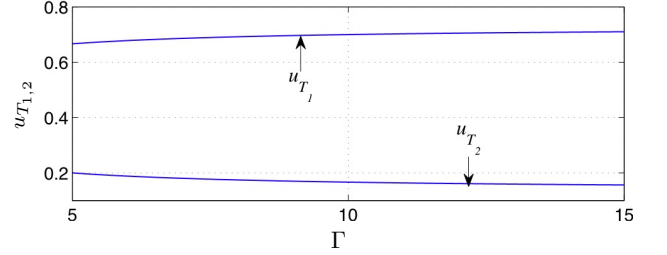


FIG. 13: The variation of two tangent points  $u_{T1,2}$  with respect to  $\Gamma$ .

1.  $u_{c-1}$  is the “distal” side of the critical cell  $c$ . It stays in its higher equilibrium since the wave back can not pass it. Thus we can approximately determine it by finding the biggest crossing point between two nullclines. In the wave back case, because  $u_{T1}$  is close to the higher equilibrium,  $\Delta U_{c-1}$  is nearly zero. Then we determine  $u_{c-1}$  as 0.9. In the wave front case, however,  $u_{T2}$  is small. Considering the minus  $\Delta U_{c-1}$ , we determine  $u_{c-1}$  as 0.8.
2.  $u_{c+1}$  is the “proximal” side of the critical cell  $c$ . It switches off before cell  $c$  when wave backs come and waits to be excited again by cell  $c$ , so at the critical time,  $u_{c+1}$  closes to 0.
3. In Fig. 13, we draw  $u_{T1,2}$  according to Eq. 14. Obviously,  $u_{T1}$  and  $u_{T2}$  change little so that they can be regarded as constants 0.7 and 0.17, respectively.
4. Note that above approximations do not stand when coupling strength is too large.

According to above approximations, substituting

$$u_{T1} = 0.7, u_{c-1} = 0.9, u_{c+1} = 0$$

into Eq. 15, and

$$u_{T2} = 0.17, u_{c-1} = 0.8, u_{c+1} = 0$$

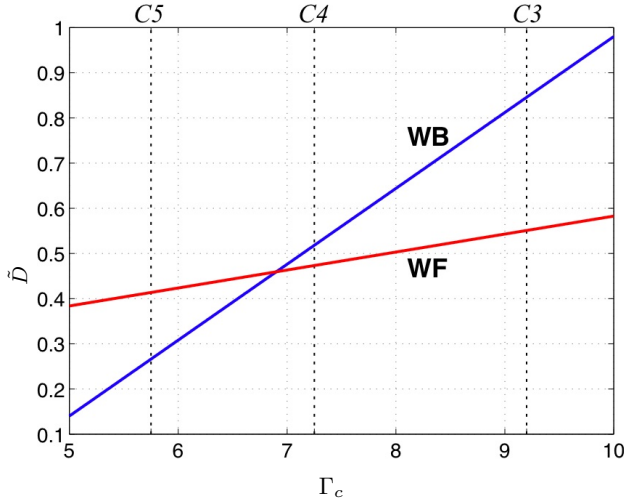


FIG. 14: The diagram in  $(\Gamma_c, \tilde{D})$  parameter plan representing the conditions of collective oscillation. We have wave back to pass the cell, and wave front to reflect, when parameters locat above the blue (WB) and red (WF) line, respectively.

into Eq. 16, we get two rough conditions

$$0.084\Gamma_c - 0.5\tilde{D} < 0.35 \quad \text{WB passes,} \quad (17)$$

$$-0.0183\Gamma_c + 0.46\tilde{D} > 0.085 \quad \text{WF generates.} \quad (18)$$

Clearly the critical coupling strength increases linearly with respect to active factor  $\Gamma$ . We draw two lines in Fig. 14, where blue (WB) and red (WF) lines are obtained from Eq. 17 and Eq. 18, respectively. In Fig. 14,  $C3$ ,  $C4$  and  $C5$  on top horizontal axis indicate the value of  $\Gamma$  defined by Eq. 4 for cell 3, 4 and 5, respectively. Lines WF and WB cross to each other between  $C4$  and  $C5$ . This kind of topology makes  $4^{th}$  and  $5^{th}$  cell to behave completely different.

For cell 5, WF is above WB. If coupling strength is between WF and WB, the wave back coming from center can switch  $4^{th}$  cell off, but the cell is no able to be switched on to fire a wave front. This is exactly the situation shown in Fig. 5, in which no oscillation takes place. On the other hand, in the case of cell 4, WF is below WB. Clearly, if a coupling strength allows the wave back

to repress  $4^{th}$ , the cell will be excited again and lead to a wave front.

The conditions for these two situations are dependent on many other elements, such as initial conditions, propagating velocity, cell excitability, and so on. It is much more complicated than the approximated case we discussed here. Qualitatively, we can conclude that the tuning point of these two condition lines is the origin of self-sustained collective oscillation.

## V. CONCLUDING REMARKS

In this paper, we proposed a brand-new scenario for self-organized and self-sustained oscillation in a multicellular biological tissue. Distinct from current framework based on oscillatory genetic network, there is no self-oscillatory cell and periodic external stimulation in the system. In contrast, coupling a number of cells together gives rise to collective oscillation inside the cell group, i.e., a tissue. Moreover, the oscillation can manifests itself in several ways, corresponding to different coupling strength. Anti-phase and In-phase oscillations occurring on two boundaries lead to the alternative change of oscillating position and oscillating cell population, respectively. The birth and death of oscillation resulting from the variation of coupling strength are also discussed. On the other hand, we give a general idea on how the size of field, in which cells grow, effects the oscillatory behavior. It is of interest to extent our new hypothesis to spatial three dimensional systems, as a more realistic model of living organism. Finally, a detailed investigation of dynamical movement of nullcline provides the insight of the mechanism of complicated oscillatory phenomena. Although there have appeared several studies on the self-oscillatory phenomenon in spatially discretized systems in the context of mathematics and physics, this paper introduce these basic idea to the spatio-temporal self-organization in biology system.

Our observation have been undergone by numerical simulation. As the next step, analytical studies inspired by these interesting phenomenon are awaited. We are going to design corresponding biological experiments and to explore more proofs supporting our hypothesis.

- 
- [1] U. Schibler and F. Naef, Current Opinion in Cell Biology **17**, 223 (2005).
  - [2] O. Pourquie, Science **301**, 328 (2003).
  - [3] J. Stark, C. Chan, and A. J. T. George, Immunological Reviews **216**, 213 (2007).
  - [4] G. Tian, S. Krishna, S. Pigolotti, M. H. Jensen, and K. Sneppen, Physical Biology **4**, R1 (2007).
  - [5] H. Hirata, S. Yoshiura, T. Ohtsuka, Y. Bessho, T. Harada, K. Yoshikawa, and R. Kageyama, Science **298**, 840 (2002).
  - [6] A. Hoffmann, A. Levchenko, M. L. Scott, and D. Baltimore, Science **298**, 1241 (2002).
  - [7] J. Lewis, Current Biology **13**, 1398 (2003).
  - [8] L. Chen and K. Aihara, Circuits and Systems I, IEEE Transactions on **49**, 1429 (2002).
  - [9] Y. Masamizu, T. Ohtsuka, Y. Takashima, H. Nagahara, Y. Takenaka, K. Yoshikawa, H. Okamura, and R. Kageyama, PNAS **103**, 1313 (2006).
  - [10] D. Gonze and A. Goldbeter, Chaos **16**, 026110 (2006).
  - [11] J. Garcia-Ojalvo, M. Elowitz, and S. Strogatz, PNAS **101**, 10955 (2004).
  - [12] J. S. O'Neill, E. S. Maywood, J. E. Chesham, J. S. Tak-

- hashi, and M. H. Hastings, *Science* **320**, 949 (2008).
- [13] T. Yanagita, Y. Nishiura, and R. Kobayashi, *Physical Review E* **71**, 036226 (2005).
  - [14] O. Nekhamkina and M. Sheintuch, *Physical Review E* **73**, 066224 (2006).
  - [15] S. Smale, in *The Hopf Bifurcation and Its Application*, edited by J. E. Marsden and M. McCracken (Springer-Verlag, NY, 1974), chap. 11.
  - [16] A. Y. Pogromsky, *International Journal of Bifurcation and Chaos* **8**, 295 (1998).
  - [17] A. Pogromsky, T. Glad, and H. Nijmeijer, *International Journal of Bifurcation and Chaos* pp. 629–644 (1999).
  - [18] A. Gomez-Marin, J. Garcia-Ojalvo, and J. M. Sancho, *Physical Review Letters* **98**, 168303 (2007).
  - [19] P. Couillet, J. Lega, B. Houchmanzadeh, and J. Lajzerowicz, *Physical Review Letters* **65**, 1352 (1990).
  - [20] A. Hagberg and E. Meron, *Chaos* **4**, 477 (1994).
  - [21] M. Bode, *Physica D: Nonlinear Phenomena* pp. 270–286 (1997).
  - [22] A. Prat and Y. Li, *Physica D: Nonlinear Phenomena* pp. 50–68 (2003).
  - [23] A. Prat, Y. Li, and P. Bressloff, *Physica D: Nonlinear Phenomena* pp. 177–199 (2005).
  - [24] Y. Li, *Physica D: Nonlinear Phenomena* pp. 27–49 (2003).
  - [25] J. Miyazaki and S. Kinoshita, *Physical Review E* **76**, 066201 (2007).
  - [26] N. M. Shnerb, Y. Louzoun, E. Bettelheim, and S. Solomon, *PNAS* **97**, 10322 (2000).
  - [27] J. P. Keener, *SIAM J. Appl. Math.* **47**, 556 (1987).
  - [28] A. M. Turing, *Philos. Trans. R. Soc. London* **B327**, 37 (1952).
  - [29] R. Kageyama, Y. Masamizu, and Y. Niwa, *Developmental Dynamics* **236**, 1403 (2007).
  - [30] M. Ibanes and J. C. I. Belmonte, *Molecular Systems Biology* **4** (2008).
  - [31] D. Ben-Zvi, B.-Z. Shilo, A. Fainsod, and N. Barkai, *Nature* **453**, 1205 (2008).
  - [32] L. Wolpert, *J. Theoret. Biol.* **25**, 1 (1969).
  - [33] P. Ashwin and M. Timme, *Nature* **436**, 36 (2005).
  - [34] D. Angeli, J. James E. Ferrell, and E. D. Sontag, *PNAS* **101**, 1822 (2007).
  - [35] J. M. A. M. Kusters, J. M. Cortes, W. P. M. van Meerwijk, D. L. Ypey, A. P. R. Theuvenet, and C. C. A. M. Gielen, *Physical Review Letters* **98**, 098107 (2007).
  - [36] H. Maamar, A. Raj, and D. Dubnau, *Science* **317**, 526 (2007).
  - [37] J.-R. Kim, Y. Yoon, and K.-H. Cho, *Biophysical Journal* **94**, 359 (2008).
  - [38] L. J. Holt, A. N. Krutchinsky, and D. O. Morgan, *Nature* **454**, 353 (2008).
  - [39] F. Luckel, K. Kubo, K. Tsumoto, and K. Yoshikawa, *FEBS Letters* **579**, 5119 (2005).
  - [40] N. Makita and K. Yoshikawa, *FEBS Letters* **460**, 333 (1999).
  - [41] K. Tsumoto and K. Yoshikawa, *Biophysical Chemistry* **82**, 1 (1999).
  - [42] Y. S. Mamasakhlisov, S. Hayryan, V. F. Morozov, and C.-K. Hu, *Physical Review E* **75**, 061907 (2007).
  - [43] P. Schanda, V. Forge, and B. Brutscher, *PNAS* **104**, 11257 (2007).
  - [44] S. Etienne-Manneville and A. Hall, *Nature* **420**, 629 (2002).